

Systematics of Heavy Ion Radiotherapy

J.J. Bevelacqua, Bevelacqua Resources

Abstract

Heavy ion therapy has been successful in localizing the radiation dose at a tumor site. For example, ^{12}C ion therapy not only permits dose localization, but the ^{10}C and ^{11}C positron emitting beam fragments also facilitate *in-situ* monitoring of the beam via positron emission tomography (PET). Beam localization and PET monitoring of beam fragmentation products are not unique to ^{12}C , but are shown to be general characteristics of heavy ions that occur across the Periodic Table.

Keywords

Basic Health Physics Principles
Depth Dose Profile
Heavy Ion Stopping Power
Heavy Ion Therapy

Introduction

The systematics of the interaction of heavy ions with media are described by well-known relationships.^[1-9] When applied to therapy applications, these systematics offer significant potential because the physics of heavy ion stopping power permits the dose to be localized. It is well established^[6] that the fragmentation products of a ^{12}C ion beam include the ^{10}C and ^{11}C positron emitters. By monitoring the electron – positron annihilation by positron emission tomography (PET), the ^{12}C ion dose distribution can be determined.^[6] The ability to localize the dose and to monitor the beam profile *in-situ* are positive aspects of heavy ion therapy.

This article will show that the capability to localize and monitor the beam is not restricted to ions such as ^{12}C , but is a characteristic that exists throughout the periodic table. Heavy ion ranges for ^4He , ^{12}C , ^{16}O , ^{20}Ne , ^{40}Ca , ^{63}Cu , ^{92}Mo , ^{107}Ag , ^{142}Nd , ^{172}Hf , ^{184}Os , ^{197}Au , ^{209}Bi , ^{238}U , and ^{236}Np are calculated to illustrate the localization phenomena. As applicable, a listing of candidate positron emitting beam fragments is provided for these heavy ions. In addition, the formalism to calculate the dose equivalent as a result of heavy ion therapy is illustrated.

Prior to reviewing the methodology for determining the ion's range, an overview of external beam therapy and heavy ion therapy is outlined. This overview provides a basis for a more detailed examination of heavy ion therapy systematics.

Overview of External Beam Therapy

External beam therapy for the treatment of disease such as cancer can be accomplished using a variety of radiation types including photons, electrons, protons, and heavy ions.^[1-3] For photon beams, divergence and attenuation reduce the photon fluence as a function of the depth in tissue.

However, the electron density builds to an equilibrium value inside the tissue. The combination of these effects produces a dose equivalent curve that rises to a maximum and then decreases with increasing depth into the tissue. Electron backscatter increases the surface dose equivalent to a value between 15 - 100 % of the maximum dose. The depth of the maximum dose equivalent increases with increasing beam energy. For example, the dose equivalent curve for 15 MeV photons peaks at about 2.7 cm depth and clinically useful radiation is available beyond 10 cm tissue depth.

With electron beams, the primary electrons slow down in tissue and produce high ionizations per unit length as they reach their maximum range. For tissue depths beyond the maximum range, the electron dose equivalent decreases very rapidly to a value of only a few percent of the maximum dose equivalent. The stopping power for high-energy electrons is about 2 MeV/cm in tissue and about twice this value in bone.

For electron energies below 1 MeV, the maximum dose equivalent occurs near the skin surface. Since most lesions are below the surface of the skin, it is advantageous to use higher energy beams. By properly selecting the beam energy the tumor is attacked while the underlying tissue is spared. For example, a chest wall tumor should be treated without damaging the underlying lung tissue. As the electron beam energy increases from 4 to 20 MeV, the shape of the dose equivalent curve shifts from a surface peak to a broader plateau extending into tissue. Beyond 20 MeV, the plateau expands, and the advantage of sparing healthy tissue at depth is lost. In general, the useful electron energy range is between 4 and 20 MeV.

Proton beams produce a relatively low constant dose equivalent that terminates in a narrow peak at the end of the dose equivalent curve. The dose equivalent can be highly localized which produces high tumor energy deposition and lower healthy tissue dose equivalents. However, the ability to track a conventional beam is limited. Tracking is important to ensure the entire tumor volume is irradiated.

A tumor may be approximated as a central mass with numerous protrusions or microextensions extending outward in random directions. In order to destroy the tumor both the central mass and the microextensions must be

destroyed. A highly localized beam could destroy the central tumor mass, but leave the microextensions relatively intact and capable of further growth. Therefore, some spreading in the dose equivalent profile is desirable.

An optimum therapy approach must have the capability to localize and track the beam to ensure it irradiates the entire tumor volume. Prior to addressing these characteristics, an overview of heavy ion therapy and its physical basis is provided.

Introduction to Heavy Ion Therapy

Conventional beam radiotherapy with photons and electrons is limited because healthy tissue is irradiated during tumor irradiation. In order to overcome the physical and biological limitations of conventional radiotherapy, the use of heavy charged particles or heavy ions was proposed by Wilson.^[4] The use of heavy ions allows the deposition of a higher dose equivalent to a deep-seated tumor than proton therapy. This is accomplished because heavy ions exhibit an inverse dose equivalent profile with dose equivalent increasing with penetration depth and maximum dose equivalent occurring at the Bragg peak.^[1-6,9]

For deep-seated tumors, an ideal therapy protocol would involve the selective deposition of energy at the tumor site with minimal deposition to locations outside the tumor mass. As noted by Kraft,^[6] heavy ions such as ¹²C would exhibit a low relative biological effectiveness (RBE) near the body surface with a good likelihood for healthy tissue repair. In comparison, a strongly elevated RBE would occur near the end of the heavy ion's range and the damaged deoxyribonucleic acid (DNA) in this region is more difficult to repair. This is an ideal therapy condition because the healthy tissue receives a smaller dose equivalent than the tumor, and it will exhibit a greater likelihood for repair.

As the heavy ion mass increases beyond carbon, higher RBEs (relative to carbon) result in the healthy tissue in the entrance area. The entrance RBE increases with increasing atomic number of the heavy ion beam.^[6] Since the RBE impacts the effectiveness of the repair of damaged DNA, the repair capability of the irradiated tissue becomes relevant. Healthy tissue repair is an important consideration for slowly growing tumors that have a significant repair capacity and

are usually radioresistant. Using an ion such as ^{12}C with a relatively low entrance RBE facilitates healthy tissue repair, and if the Bragg peak is placed within the tumor volume large RBE values occur at the desired location. This is a primary motivation for treating tumors with ^{12}C .

When compared to protons, heavy ions (e.g., ^{12}C ions) have a larger RBE, smaller lateral scattering, and smaller range straggling.^[6] The primary heavy ion beam will suffer a small amount of fragmentation. In the case of ^{12}C , this fragmentation produces other ions such as ^{10}C and ^{11}C . The fragmentation produces additional dose equivalent beyond the Bragg peak, but it also has a positive effect. The fragmentation ions include positron emitters that can be detected using positron emission tomography. PET permits monitoring the distribution of positron emitters and consequently the primary heavy ions are monitored and compared to the planned therapy dose equivalent distribution.^[6] The increased RBE at the tumor site, improved dose equivalent distribution, and possibility of PET monitoring are clear advantages of heavy ions over conventional protons, electrons, and photons.

Physical Basis for Heavy Ion Beam Therapy

As noted earlier, the primary motivation for the use of heavy ion beam therapy is the inverse depth dose curve. For energies relevant to therapy applications of several hundred MeV/amu, the stopping power ($-dE/dx$) of an ion is dominated by electronic collisions. Using relativistic quantum mechanics, Bethe derived the following equation for the stopping power in a uniform medium for a heavy charged particle or heavy ion^[5-7]:

$$-\frac{dE}{dx} = \frac{4\pi k^2 z^2 e^4 n}{mc^2 \beta^2} \left[\ln \frac{2mc^2 \beta^2}{I(1-\beta^2)} - \beta^2 \right] \quad (\text{Eq. 1})$$

where

k = electric constant = $8.99 \times 10^9 \text{ N}\cdot\text{m}^2/\text{C}^2$;

z = atomic number of the heavy ion;

e = magnitude of the electric charge = $1.6 \times 10^{-19} \text{ C}$;

n = number of electrons per unit volume in the medium interacting with the heavy ion;

m = electron rest mass = $9.11 \times 10^{-31} \text{ kg}$;

c = velocity of light in a vacuum

= $3.00 \times 10^8 \text{ m/s}$;

β = velocity of the particle relative to the speed of light = v/c ;

v = velocity of the heavy ion; and

I = mean excitation energy of the medium interacting with the heavy ion.

Using relativistic mechanics, β can be determined from the total energy (W) and rest energy (E_o).^[3,5,8]

$$W = E + E_o \quad (\text{Eq. 2})$$

$$E_o = m_o c^2 \quad (\text{Eq. 3})$$

$$W = \frac{m_o c^2}{\sqrt{1-\beta^2}} \quad (\text{Eq. 4})$$

where E is the ion's kinetic energy and m_o is the ion's rest mass. Using Equations 2 – 4 leads to an expression for the ion's kinetic energy:

$$E = W - E_o = m_o c^2 \left(\frac{1}{\sqrt{1-\beta^2}} - 1 \right) \quad (\text{Eq. 5})$$

Equation 5 can be solved for β :

$$\beta = \left[1 - \left(\frac{m_o c^2}{E + m_o c^2} \right)^2 \right]^{1/2} = \left[1 - \left(\frac{E_o}{W} \right)^2 \right]^{1/2} \quad (\text{Eq. 6})$$

for use in Equation 1.

The mean excitation energy I can be represented by the following empirical formulas for an element with atomic number Z ^[5]:

$$I \cong 19.0eV, Z = 1 \quad (\text{Eq. 7})$$

$$I \cong (11.2 + 11.72Z)eV, 2 \leq Z \leq 13 \quad (\text{Eq. 8})$$

$$I \cong (52.8 + 8.71Z)eV, Z > 13 \quad (\text{Eq. 9})$$

Once the stopping power is known, it is possible to calculate the ion's range. The range of a charged particle is the distance it travels before coming to rest. The reciprocal of the stopping power is the distance traveled per unit energy loss. Therefore, the range $R(E)$ of a charged particle having kinetic energy E is the integral of the

reciprocal of the negative stopping power from the initial kinetic energy E_i to the final kinetic energy of a stopped particle ($E = 0$):

$$R(E) = \int_{E_i}^0 (dE / dx)^{-1} dE \quad (\text{Eq. 10})$$

Equation 10 is often written in terms of the stopping power:

$$R(E) = \int_0^{E_i} (-dE / dx)^{-1} dE \quad (\text{Eq. 11})$$

As the heavy ion beam loses energy, it broadens in a variety of ways including energy, position, and angle. For example, the Bragg peak spreads in energy and has a distinctive width. Each of these spreading mechanisms affects the delivered dose equivalent at the tumor site. Accordingly, energy straggling, range straggling, and angle straggling are briefly addressed.

For a beam of heavy ions, the width of the Bragg peak is caused by the summation of multiple scattering events that yield a Gaussian energy loss distribution often referred to as energy straggling^[8]:

$$\frac{N(E)dE}{N} = \frac{1}{\alpha\pi^{1/2}} \exp\left[-\frac{(E - \bar{E})^2}{\alpha^2}\right] \quad (\text{Eq. 12})$$

Energy straggling represents the specific number $N(E)$ of particles having energies in the range E to $E + dE$ divided by the number of particles N , with mean energy \bar{E} after traversing a thickness x_o of absorber. The distribution parameter or straggling parameter (α) expresses the half-width at the $(1/e)$ -th height and is given by the expression^[8]:

$$\alpha^2 = 4\pi z^2 e^4 n Z x_o \left[1 + \frac{KI}{m v^2} \ln\left(\frac{2m v^2}{I}\right) \right] \quad (\text{Eq. 13})$$

where K is a constant depending on the electron shell structure of the absorber and has a value between $2/3$ and $4/3$ and Z is the atomic number of the absorber. It is also possible^[6,9] to recast Equation 13 to represent the full width at half-maximum (FWHM) height.

In an analogous manner, the range straggling, expressed as the number of particles $N(R)$ with

ranges R to $R + dR$ divided by the total number of particles of the same initial energy, is given by the equation^[8]:

$$\frac{N(R)dR}{N} = \frac{1}{\alpha\pi^{1/2}} \exp\left[-\frac{(R - \bar{R})^2}{\alpha^2}\right] \quad (\text{Eq. 14})$$

where \bar{R} is the mean range.

Upon entering a medium of thickness x_o , a collimated beam experiences multiple collisions that broaden the beam and cause it to diverge. This phenomena is called angle straggling, and the mean divergence angle ($\bar{\theta}$) is given by the relationship^[8]:

$$\bar{\theta}^2 = \frac{2\pi z^2 e^4}{E^2} n Z^2 x_o \ln\left(\frac{\bar{E} a_o}{z Z^{4/3} e^2}\right) \quad (\text{Eq. 15})$$

where a_o is the Bohr radius:

$$a_o = \frac{\hbar^2}{km e^2} \quad (\text{Eq. 16})$$

Range Calculations

Heavy ion range calculations are provided in this section. Since range is being calculated, the relationship between the range and the peak of the dose equivalent distribution needs to be established. To accomplish this, the effects of straggling are briefly considered.

The position of the Bragg peak and straggling full width at half-maximum are summarized in Table 1. The values are provided for ^{12}C ions with energies between 90 and 330 MeV/amu.^[9] Table 1 indicates that the particle range is a reasonable approximation to the Bragg peak for heavy ions.

The values in parenthesis in Table 1 are the results for Stopping Powers and Ranges (SPAR) Code calculations^[10] to verify the model used in this article. SPAR includes a somewhat different formulation of the stopping power than utilized in this article, but it is sufficient to verify the validity of our calculations. The differences in the calculated ranges arise from SPAR's parameterization of the mean ionization and the inclusion of shell-effect and density-effect corrections. In addition, SPAR utilizes approximations that become less valid as the ion's atomic number increases beyond about 50.

Table 1. ¹²C Ion Range and Straggling Widths in Water

Energy (MeV/amu)	Range @ Peak Position (cm) ^a	Straggling FWHM (cm) ^a	Range (cm) This Work ^b
90	2.13	0.07	2.14 (2.12)
198	8.28	0.23	8.54 (8.45)
270	14.43	0.5	14.5 (14.3)
330	20.05	0.7	20.2 (19.9)

^a Ref. 9, U. Weber (1996).

^b Values in parenthesis are based on the SPAR Code, Ref. 10.

Table 2. Heavy Ion Ranges in Water (cm) for Selected Energies

Ion	Ion Energy (MeV/amu)			
	90	198	270	330
⁴ He	6.42	25.6	43.4	60.5
¹² C	2.14	8.54	14.5	20.2
¹⁶ O	1.60	6.40	10.8	15.1
²⁰ Ne	1.28	5.12	8.67	12.1
⁴⁰ Ca	0.64	2.56	4.34	6.05
⁶³ Cu	0.48	1.92	3.25	4.53
⁹² Mo	0.34	1.34	2.26	3.15
¹⁰⁷ Ag	0.31	1.24	2.10	2.93
¹⁴² Nd	0.25	1.01	1.71	2.38
¹⁷² Hf	0.21	0.85	1.44	2.01
¹⁸⁴ Os	0.20	0.82	1.38	1.93
¹⁹⁷ Au	0.20	0.81	1.37	1.91
²⁰⁹ Bi	0.19	0.78	1.32	1.83
²³⁸ U	0.18	0.72	1.22	1.70
²³⁶ Np	0.18	0.70	1.18	1.65

Since one of the purposes of this article is the calculation of the range of heavy ions, Table 2 provides the results of calculations of the range in water for a number of heavy ions including ⁴He, ¹²C, ¹⁶O, ²⁰Ne, ⁴⁰Ca, ⁶³Cu, ⁹²Mo, ¹⁰⁷Ag, ¹⁴²Nd, ¹⁷²Hf, ¹⁸⁴Os, ¹⁹⁷Au, ²⁰⁹Bi, ²³⁸U, and ²³⁶Np. The ions ranges are evaluated for energies between 90 and 330 MeV/amu, and we assume that water is a reasonable approximation for the tissue composition.

The results of Table 2 illustrate that desired irradiation locations can be achieved by selecting specific ion and energy combinations. This characteristic is highly desirable in providing an effective treatment protocol. The ability to target a specific location by selecting the ion and its energy makes heavy ions an attractive tool for therapy applications.

The ion range estimate is a preliminary step in formulating a therapy protocol. Therapy planning also involves an estimate of delivered dose and the distribution of that dose within the tumor volume.

A method for the determination of the dose is outlined in the next section of this article. This approach can also be used to determine the dose distribution. The *in-situ* determination of the dose distribution will be discussed following the presentation of the dose methodology.

Absorbed Dose from a Heavy Ion Beam

For a volume irradiated by a parallel beam of particles, the absorbed dose (D) as a function of penetration distance x into this volume is given by:

$$D(x) = \frac{1}{\rho} \left(-\frac{dE}{dx} \right) \Phi(x) \quad (\text{Eq. 17})$$

where ρ is the density of the material (tissue or tumor) attenuating the heavy ion, $-dE/dx$ is the stopping power, and Φ is the heavy ion fluence. The particle fluence varies with penetration distance according to the relationship:

$$\Phi(x) = \Phi(0) \exp(-\mu x) \quad (\text{Eq. 18})$$

where $\Phi(0)$ is the entrance fluence and μ is the macroscopic reaction cross-section (linear attenuation coefficient). The linear attenuation coefficient is defined as

$$\mu = N\sigma \quad (\text{Eq. 19})$$

where N is the number of atoms of absorbing material per unit volume and is σ the total microscopic reaction cross-section for the heavy ion-tissue interaction.

For practical radiotherapy applications, the energy of the primary beam is varied to alter the Bragg peak position. By varying the energy, the tumor volume can be irradiated with a series of overlapping Bragg peaks.

In principle, the dose distribution from each beam can be summed to obtain the total dose distribution. However, in performing this sum the absorbed dose must be modified by a radiation weighting factor that is energy dependent. Kraft [6] notes that for ^{12}C the RBE initially increases by factors of 2 – 4 when the heavy ion slows. From a practical standpoint, the complex heavy ion interaction sequence must be known when variations of RBE and radiation weighting factor are included in dose specification and optimization.

When calculating the dose equivalent to a complex medium such as tissue, the methodology must be modified. In particular, modifications to the linear attenuation coefficient and stopping power are required.

For a medium, such as tissue [5] composed of hydrogen (5.98×10^{22} atoms/cm³), oxygen (2.45×10^{22} atoms/cm³), carbon (9.03×10^{21} atoms/cm³), and nitrogen (1.29×10^{21} atoms/cm³), the attenuation coefficient is given by the summation over each of its component element attenuation coefficients times their number density:

$$\mu = \sum_i \mu_i N_i \quad (\text{Eq. 20})$$

In a similar fashion, the stopping power for a medium composed of a number of elements i having charge Z_i , number density N_i , and mean excitation I_i is obtained through a modification of Equation 1. In particular for a complex medium, the following substitution is made in Equation 1 [5]:

$$n / \ln I \rightarrow \sum_i N_i Z_i / \ln I_i \quad (\text{Eq. 21})$$

In-situ Determination of the Dose Distribution through Nuclear Fragmentation

When a heavy ion beam interacts with tissue, the interactions leave nuclei in an excited state, and these excited nuclei decay by a variety of processes including particle emission and deexcitation by photon emission. These secondary fragments must be considered in therapy dose planning because they broaden the Bragg peak.

As an example, consider a therapy protocol in which primary ^{16}O ions impinge on tissue and a portion of the beam produces ^{15}O and neutron fragments. The delivered dose equivalent (H) will be composed of 3 components:

$$H = H(^{16}\text{O}) + H(^{15}\text{O}) + H(n) \quad (\text{Eq. 22})$$

where the first term accounts for the ^{16}O dose equivalent from the primary beam. The ^{16}O fluence decreases as it penetrates tissue

$$\Phi(^{16}\text{O}, x) = \Phi(^{16}\text{O}, 0) \exp(-\mu x) \quad (\text{Eq. 23})$$

where μ is the ^{16}O total macroscopic reaction cross-section. The second and third terms in Equation 22 are the dose equivalent contributions that arise from the fragmentation of $^{16}\text{O} \rightarrow ^{15}\text{O} + n$. The neutron and ^{15}O fluence depend on a number of factors including the ^{16}O fragmentation cross-section as a function of energy and angle, the ^{15}O and neutron reaction cross-sections, and the energy dependent tissue interactions.

The dose distribution depends on the number of primary beam particles, fragments, and deexcitation products. For each component, the energy, interaction angular distribution, and RBE are key aspects of therapy dose planning. In particular, the increased entrance RBE to healthy tissue that occurs with increasing ion atomic number must be balanced against the larger RBE values that occur at the tumor site. The optimum ion and energy will depend on the specific tumor characteristics. However, higher Z ions should be evaluated to optimize therapy dose delivery.

One of the key aspects of the delivered dose is the beam's spatial distribution. The spatial distribution can be measured by monitoring the positron-electron annihilation photons resulting from primary beam fragmentation products. For the Equation 22 example, ^{15}O would provide a measure of the beam profile by monitoring the annihilation of the emitted positrons using PET. The next section of this article reviews the

production of positron emitters for a variety of candidate ion beams.

Production of Positron Emitting Isotopes

Beam fragmentation has a positive aspect in that it introduces the possibility for *in-situ* beam observation using positron emission tomography. For example, a common fragmentation mode is the stripping of neutrons from the primary ion. Neutron stripping moves a nucleus away from the line of stability, increases the proton to neutron ratio, and naturally leads to a positron emitter.

Table 3 provides candidate heavy ion therapy beams and their possible PET fragmentation products. For simplicity, Table 3 considers the most likely positron emitting fragments that occur by neutron removal from the primary beam ion. The results of Table 3 indicate that heavy ion beams from elements spanning the entire Periodic Table can be monitored using PET techniques to ensure the beam's effectiveness in tumor irradiation. The information in Table 3 was derived from Reference 11.

Primary Ion	Positron Emitting Fragmentation Products^a	Positron Emitting Fragmentation Product Half-Life
⁴ He	-----	-----
¹² C	⁹ C	127 ms
	¹⁰ C	19.3 s
	¹¹ C	20.3 m
¹⁶ O	¹³ O	8.9 ms
	¹⁴ O	70.6 s
	¹⁵ O	122 s
²⁰ Ne	¹⁷ Ne	109 ms
	¹⁸ Ne	1.67 s
	¹⁹ Ne	17.2 s
⁴⁰ Ca	³⁵ Ca	0.05 s
	³⁶ Ca	~0.1 s
	³⁷ Ca	173 ms

	³⁸ Ca	0.44 s
	³⁹ Ca	861 ms
Table 3. Candidate Heavy Ion Fragmentation Products that Can Be Monitored Using PET		
Primary Ion	Positron Emitting Fragmentation Products^a	Positron Emitting Fragmentation Product Half-Life
⁶³ Cu	⁶² Cu	9.74 m
	⁶¹ Cu	3.35 h
	⁶⁰ Cu	23.7 m
	⁵⁹ Cu	1.36 m
	⁵⁸ Cu	3.21 s
⁹² Mo	⁹¹ Mo	15.5 m
	^{91m} Mo	1.08 m
	⁹⁰ Mo	5.7 h
	⁸⁹ Mo	2.2 m
	⁸⁸ Mo	8 m
	⁸⁷ Mo	14 s
¹⁰⁷ Ag	¹⁰⁶ Ag	24.0 m
	¹⁰⁵ Ag	41.3 d
	¹⁰⁴ Ag	1.15 h
	^{104m} Ag	33 m
	¹⁰³ Ag	1.1 h
	¹⁰² Ag	13.0 m
	^{102m} Ag	7.8 m
¹⁴² Nd	¹⁴¹ Nd	2.49 h
	^{141m} Nd	1.04 m
	¹³⁹ Nd	30 m
	^{139m} Nd	5.5 h
	¹³⁷ Nd	38 m
¹⁷² Hf	¹⁷¹ Hf	12.2 h
	¹⁶⁹ Hf	3.25 m
	¹⁶⁸ Hf	25.9 m
	¹⁶⁷ Hf	2 m

Table 3. Candidate Heavy Ion Fragmentation Products that Can Be Monitored Using PET

Primary Ion	Positron Emitting Fragmentation Products ^a	Positron Emitting Product Half-Life
¹⁸⁴ Os	¹⁸³ Os	13 h
	¹⁸¹ Os	2.7 m
	^{181m} Os	1.75 h
	¹⁷⁹ Os	7 m
¹⁹⁷ Au	¹⁹⁶ Au	6.18 d
	¹⁹⁴ Au	1.64 d
	¹⁹² Au	4.9 h
²⁰⁹ Bi	²⁰⁷ Bi	32.2 y
	²⁰⁶ Bi	6.24 d
	²⁰⁵ Bi	15.3 d
²³⁸ U	-----	-----
²³⁶ Np	²³⁴ Np	4.4 d

^a The fragmentation products are limited to the loss of 5 neutrons from the primary ion to display the most likely nuclides.

An examination of Table 3 suggests that *in-situ* beam monitoring via PET is possible throughout most of the Periodic Table. However, it becomes more difficult as the mass increases beyond about A = 200.

Determination of Total Reaction Cross-Section

Equation 19 uses the total microscopic reaction cross-section to obtain the total macroscopic reaction cross-section. The total microscopic reaction cross-section can be obtained from parameterizations of Shen and coworkers [12] or the use of optical model codes such as DWUCK [13] or MERCURY [14-16]

Shen's model is a parametric fit to available cross-section data using established relationships including trends in nuclear radii, reaction kinematics, and energy dependence. The optical model codes require parameterization of the entrance and exit channel reactions, nuclear

structure information for the transferred particles, spectroscopic information, and specification of kinematic information related to the reaction under investigation. Each of these approaches has its inherent shortcomings and these must be clearly understood. The best practice is to use measured data. However, the use of models is often required because a complete set of cross-sections are often not available.

Final Considerations

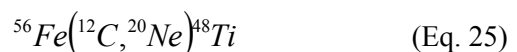
There are options for maximizing the delivery of dose to a tumor from heavy ions with $Z > 6$, while limiting the dose to healthy tissue. These options depend on developing technology that is not yet fully available, and include:

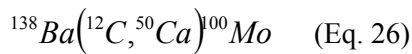
- The use of nanotechnology to deliver the heavy ion beam from within the tumor without penetrating healthy tissue. As noted in Table 2, a 90 MeV/amu ¹⁹⁷Au beam has a range of about 0.2 cm in water. A series of nanoaccelerators implanted within the tumor mass would effectively irradiate the desired volume while limiting the dose to healthy tissue.
- The use of a radioprotective agent that is preferentially absorbed by healthy tissue. This agent would mitigate the higher entrance RBE values that occur for $Z > 6$ ion beams, and reduce the dose to healthy tissue.

- The use of a chemical agent that is preferably absorbed by the tumor. Such an agent would include an element X tagged to a bio-active molecule. By selecting an external ion beam (x), reactions of the type



would preferentially occur within the tumor mass. In Equation 24, y is the exit channel particle and Y is the residual nucleus. By selecting a reaction such that $Z_y > Z_x$, it would be possible to effectively have a high- Z ion accelerator inside the tumor. The tumor would receive dose from both the external ion beam (x) and generated internal beam (y). Examples of possible reactions for an external ¹²C ion beam include:





Equations 25 and 26 are only candidate reactions. Useful reactions for therapy applications would depend on the fluence and energy of the primary beam particle, the magnitude and energy dependence of the reaction cross-section, and the magnitude and angular dependence of the exit channel particle fluence.

Conclusions

Heavy ions have significant potential for therapy applications because careful selection of the ion and its energy permits the energy deposition to be localized. As part of the energy deposition process, the ion fragments and some of these fragments are positron emitters that result from the removal of neutrons from the primary heavy ion beam. The dose equivalent distribution can be monitored by positron emission tomography as the emitted positrons annihilate. The ability to monitor the beam is not restricted to $Z \leq 6$ ions, but is a characteristic that exists throughout the Periodic Table. The capability for dose localization and monitoring are positive aspects of heavy ions when used in therapy applications.

References

1. H. E. Johns and J. R. Cunningham, *The Physics of Radiology*, Fourth Edition, Charles C. Thomas Publisher, Springfield, IL (1983).
2. J. J. Bevelacqua, *Contemporary Health Physics, Problems and Solutions*, John Wiley & Sons, Inc., New York (1995).
3. J. J. Bevelacqua, *Basic Health Physics, Problems and Solutions*, John Wiley & Sons, Inc., New York (1999).
4. R. R. Wilson, *Radiological Use of Fast Protons*, *Radiology* **47**, 487 (1946).
5. J. E. Turner, *Atoms, Radiation, and Radiation Protection*, Second Edition, John Wiley & Sons, Inc., New York (1995).
6. G. Kraft, *Tumor Therapy with Heavy Charged Particles*, *Progress in Particle and Nuclear Physics* **45**, S473 (2000).
7. H. Bethe, *Zur Theorie des Durchgangs schneller Korpuskularstrahlung durch Materie*, *Ann. Phys. (Leipzig)* **5**, 325 (1930).
8. P. Marmier and E. Sheldon, *Physics of Nuclei and Particles*, Volume I, Academic Press, New York (1969).
9. U. Weber, *Volumenkonforme Bestrahlung mit Kohlenstoffionen*, PhD Thesis, Universität Gh Kassel, Germany (1996).
10. Radiation Safety Information Computational Center Computer Code Collection: Code Package CCC-228 SPAR, *Calculation of Stopping Powers and Ranges for Muons, Charged Pions, Protons, and Heavy Ions*, Oak Ridge National Laboratory, Oak Ridge, TN (1985), <http://rsicc.ornl.gov>, August 23, 2005.
11. *Chart of the Nuclides*, Fourteenth Edition, General Electric Company, San Jose, CA (1989).
12. W. Q. Shen, B. Wang, J. Feng, W. L. Zhan, Y. T. Zhu, and E. P. Feng, *Total reaction cross section for heavy-ion collisions and its relation to the neutron excess degree of freedom*, *Nucl. Phys. A* **491**, 130 (1989).
13. P. D. Kunz, *Computer Code DWUCK*, University of Colorado, Bolder, CO; available as part of Radiation Safety Information Computational Center Computer Code Collection: Code Package PSR-235 DWUCK, *Nuclear Model Computer Codes for Distorted Wave Born Approximation and Coupled Channel Calculations*, Oak Ridge National Laboratory, Oak Ridge, TN (1986), <http://rsicc.ornl.gov>, August 23, 2005.
14. L. A. Charlton and D. Robson, *MERCURY*, Florida State University Technical Report No. 5, Tallahassee, FL (1973).
15. L. A. Charlton, *Specific New Approach to Finite-Range Distorted-Wave Born Approximation*, *Phys. Rev.* **C8**, 146 (1973).
16. J. J. Bevelacqua, D. Stanley, and D. Robson, *Sensitivity of the Reaction $^{40}\text{Ca}(^{13}\text{C}, ^{14}\text{N})^{39}\text{K}$ to the $^{39}\text{K}+p$ Form Factor*, *Phys. Rev.* **C15**, 447 (1977).

The Author

Dr. Bevelacqua is President of Bevelacqua Resources. He is a Certified Health Physicist and received a PhD in Nuclear Physics from Florida State University. His health physics experience spans over 30 years and includes the power and research reactor, accelerator, university, nuclear fuel cycle and non-ionizing radiation areas. He has been the Radiation Protection Manager at a number of commercial nuclear power plants and held a Senior Reactor Operator Certification at a commercial pressurized water reactor. His published works include 75 journal articles, two health physics textbooks, 18 health physics training manuals, and three health physics training CD-ROMs.

Dr. Joseph Bevelacqua, PhD, CHP
Bevelacqua Resources
343 Adair Drive
Richland, WA 99352

Email: Bevelresou@aol.com